



ELSEVIER

Polymer 43 (2002) 4723–4731

**polymer**

[www.elsevier.com/locate/polymer](http://www.elsevier.com/locate/polymer)

## Co-continuous morphology development in partially miscible PMMA/PC blends

Nicolas Marin, Basil D. Favis\*

*Department of Chemical Engineering, Centre de Recherche Appliquée Sur les Polymères, École Polytechnique de Montréal, P.O. Box 6079, Station Centre-Ville, Montreal, Que., Canada H3C 3A7*

Received 28 February 2002; accepted 12 April 2002

### Abstract

Poly(methyl methacrylate) (PMMA)/polycarbonate (PC) partially miscible blends were produced via melt blending in an internal mixer over the entire range of composition at two different viscosity ratios. The morphology of this low interfacial tension system was investigated by scanning electron microscopy, solvent extraction/gravimetry and surface area measurement (BET) after selective extraction. The partial miscibility of these blends was evaluated by  $T_g$  measurements from dynamic mechanical thermal analysis. The co-continuous morphology development curve obtained from gravimetry is commonly reported in the literature as the %continuity vs. the vol% fraction of the dispersed phase for fully phase separated systems. Such systems possess pure phases of A and B. Partially miscible blends on the other hand demonstrate immiscibility between an A-rich phase and a B-rich phase. Quantitative estimation of the partial composition of the minor components in each respective rich phase was calculated using the Fox equation. Using this data, an approach to correcting the gravimetry results to take into account the partial miscibility of the PMMA/PC system is proposed. The co-continuous morphology development curve is then presented as the %continuity vs. the vol% fraction of the PMMA-rich phase. This corrected curve demonstrates the features of a highly interacting polymer blend: a low percolation threshold and a broad co-continuity region. The BET technique shows that the pore size of the extracted co-continuous blends is dependent on composition, the pore diameter increases with total PMMA content. Use of a low molecular weight PC shifts the co-continuous morphology development curve to higher volume fraction values of PMMA-rich phase. It is suggested that this is the result of a lower dispersed phase thread stability due to the lower matrix viscosity. © 2002 Elsevier Science Ltd. All rights reserved.

*Keywords:* Polymer blends; Co-continuity; Partial miscibility

### 1. Introduction

Binary polymer blends from melts show two main morphology types: dispersed phase/matrix and co-continuity. As the quantity of dispersed phase increases above the percolation threshold, the continuity of the dispersed phase increases and reaches the co-continuity region. This is characterized by an intertwining morphology of the two phases. This morphology has been intensively investigated recently [1–6,8–14].

The concept of co-continuity was first introduced as a narrow range of compositions where phase inversion occurs, also called dual phase continuity. Most studies have focussed on predicting the composition of this phase inversion. A number of models based on viscosity ratio have

been applied to this end [1–4]. The general concept of these semi-empirical models is that the less viscous phase tends to encapsulate the more viscous one. Based on the results of Avgeropoulos et al. [1], Paul and Barlow [2], reported an empirical model relating the viscosity ratio of the pure materials to the volume fraction ratio of the two phases at the phase inversion point. Later, Metelkin and Blekht [3] proposed that, at the phase inversion point, the time of break-up of a cylinder A in a matrix B should be equal to the time of break-up of a cylinder B in a matrix A. Finally, Utracki [4] demonstrated the inefficiency of these former models regarding high viscosity ratio systems. He derived a model from the theory of rigid particles suspended in a liquid and proposed that, at the phase inversion point, the viscosity of a suspension of A in B should be equal to the viscosity of suspension of B in A.

Further investigations on several systems with different viscosity ratios demonstrated that models based on viscosity

\* Corresponding author. Tel.: +1-514-340-4711; fax: +1-514-340-4159.  
E-mail address: basil.favis@polymtl.ca (B.D. Favis).

ratio often failed in predicting the phase inversion point [5]. It was clearly pointed out that encapsulation phenomena do not depend solely on the viscosity ratio.

Bourry and Favis [6] suggested an elastic contribution in the encapsulation phenomena and proposed a model based on the elasticity ratio. An elastic contribution can decrease the dynamic interfacial tension as described by Van Oene [7]. This predicts that the more elastic phase tends to encapsulate the less elastic one.

Willemse et al. [8,9] introduced a semi-empirical model, based on geometrical and microrheological considerations. This model presumably predicts both limits of the co-continuity region rather than a single phase inversion point. It was shown that increasing interfacial tension increases the onset of co-continuity for several homopolymer/homopolymer blends [9].

Compatibilized ternary blends of PE/PS/SEBS were also investigated in the co-continuity region in order to understand the influence of a copolymer (SEBS) as a compatibilizer on the co-continuity features of common uncompatibilized PE/PS blends [6,10]. It appears that the compatibilization stabilizes the co-continuity with respect to annealing [10]. It was also shown that compatibilization shifts the percolation threshold to higher amounts of dispersed phase without modifying the co-continuity region [6].

A very wide co-continuity range for a poly(ether–ester) block copolymer/polystyrene system was reported, showing that a broad range of co-continuity could be achieved in systems demonstrating a stable thread-like dispersed phase [11,12]. It was demonstrated that blending the PS and the block copolymer below its order–disorder transition temperature ensures the stability of the block copolymer dispersed phase.

Recent work from our group has studied the role of the blend interface type on co-continuous morphology. Li and Favis [13] reported the successful application of the BET nitrogen adsorption technique on measuring the mean pore diameter of selectively extracted co-continuous HDPE/PS blends. Furthermore, Li et al. [14] proposed a classification of blend interfaces which provide a general framework for the role of the interface on co-continuous morphology development. Type I systems are described as binary compatible, that is to say immiscible but demonstrating strong interactions at the interface, i.e. a low interfacial tension, and involving a stable thread-like dispersed phase even at low concentration. Consequently, the droplet lifetime during melt mixing is lower than the thread life time. Such systems attain co-continuity through thread–thread coalescence. Thus the main features of Type I systems continuity development are: (1) a low percolation threshold, (2) a broad co-continuous region and (3) the non-dependence of the pore size of extracted blends with composition.

Type II systems are immiscible and high interfacial tension blends, described as binary incompatible systems.

They commonly demonstrate a droplet dispersed phase at lower compositions, i.e. the droplet lifetime is greater than the thread life time during melt mixing. Such systems attain co-continuity through droplet–droplet coalescence. The main features of Type II systems continuity development are: (1) a higher percolation threshold than Type I, (2) a narrower co-continuous region than Type I and (3) the dependence of the dispersed phase size with composition. Finally Type III systems are ternary compatibilized blends. Such systems attain co-continuity through reduced droplet–droplet coalescence. The main features of Type III systems co-continuous morphology development are: (1) a higher percolation threshold than Type II, (2) a narrower co-continuous region than Type II and (3) the non-dependence of the dispersed phase size with the composition.

Little work has been carried out on co-continuity development in partially miscible systems. One such system is the blend of bisphenol-A polycarbonate (PC) and poly(methyl methacrylate) (PMMA). A number of studies have examined the partial miscibility of this polymer pair. It was first reported that such blends obtained via melt blending are immiscible [15,16]. In other cases, they were characterized as partially miscible [17–19]. Gardlung [19] proposed a specific interaction between the ester group of the PMMA and the benzene ring of the PC. Immiscible or miscible films can also be obtained depending on the solvent and the casting technique, i.e. air casting or non-solvent precipitation. Heptane precipitated films from tetrahydrofuran (THF) solution show miscibility and exhibit a lower critical solution temperature (LCST) behaviour (180 °C), whereas cast films from THF or methylene chloride (MC) are immiscible according to Chiou et al. [20]. Moreover Kyu and Saldanha [21–23] published numerous studies on PC/PMMA. It appears from their work that cast films from MC, cyclohexanone and THF at room temperature are immiscible, but cast films from THF at 47 °C yields miscibility and LCST behaviour (240 °C). Nishimoto et al. [24] suggested an over-estimation of miscibility due to the non-equilibrium state of miscibility of cast blends, kinetically entrapped in a homogeneous state. Indeed, they considered that no LCST behaviour above  $T_g$  for high molecular weight grades is reliable and interpreted the cloud point curve as a slow phase separation process.

Both melt and solution studies agree with the fact that PC and PMMA show partial miscibility. Kim and Burns [17] and Kolarik et al. [18] demonstrated two distinct glass transition temperatures dependant on the blend composition, given by differential scanning calorimetry and dynamic mechanical thermal analysis (DMTA). Moreover, both papers mentioned the terms PC-rich phase and PMMA-rich phase. For solution cast films, Nishimoto et al. [24] concluded that ‘even though the PC–PMMA interaction is not favourable as originally thought, it is clear that this interaction is only weakly unfavourable for mixing’. This describes not strict immiscibility nor strict miscibility, but a partial miscibility in equilibrium conditions, that is to say

immiscibility between a PMMA-rich phase, composed of PMMA and PC, and a PC-rich phase, composed of PC and PMMA.

The aim of this work is to investigate the co-continuous morphology development of a partially miscible PMMA/PC system. Comparisons will be made with systems reported recently by Li et al.

## 2. Experimental

### 2.1. Materials

Two polycarbonate grades (a general purpose grade denoted as PC1 and an high flow grade denoted as PC2) and one grade of poly(methyl methacrylate) (denoted as PMMA) were used. Several details are given in Table 1.

### 2.2. Rheology

The rheological characterization of the pure materials was carried out by plate–plate constant stress oscillation rheometry with a SR 5000 rheometer from Rheometric Scientific. The chamber was purged with dry nitrogen. Under these conditions the thermal stability at 230 °C during 1 h is excellent, i.e. the decrease in complex viscosity due to the thermal degradation is evaluated to be less than 10%. The linear domain was evaluated by stress sweep experiments in order to set the target stress of the frequency sweep experiments in the linear domain. Frequency scans were performed at about 5% deformation.

### 2.3. Melt blending

PMMA/PC1 and PMMA/PC2 blends were prepared via melt blending, using a Haake Rheocord 90 internal mixer equipped with a 78 cm<sup>3</sup> chamber and roller rotors. The temperature was set at 230 °C, the mixing time at 8 min and the rotor speed at 50 rpm. The chamber was purged with dry nitrogen and melt blends were stabilized with Ciba B225 antioxidant (0.2 wt%) and quenched in cold water after mixing. A corresponding average shear rate of 60 s<sup>-1</sup> for a rotor speed of 50 rpm in the Haake internal mixer configuration was reported by Yang et al. [25].

Table 1  
Molecular weights and densities of the pure materials

	$M_w \times 10^{-3}$ (g/mol)	$M_n \times 10^{-3}$ (g/mol)	Density (g/cm <sup>3</sup> )
PMMA	76.5	46.8	1.19
PC1	28.6	17.7	1.20
PC2	15.6	10.2	1.20

### 2.4. Scanning electron microscope

Extracted microtomed samples were prepared for qualitative analysis of the blend microstructure by SEM. First, microtomy was performed with a Leica 2165 microtome equipped with a glass knife. Then, the PMMA was selectively extracted by soxhlet extraction with formic acid for 48 h. Finally, dried samples were gold–palladium coated and SEM micrographs were obtained with a JEOL 840 microscope at 10 kV.

### 2.5. Gravimetry

Samples of each blend of about 2 mm thickness were weighed before and after selective extraction and drying (vacuum, 70 °C). The percentage of PMMA continuity is defined as

$$\%C_{\text{PMMA}} = \frac{(m_{\text{PMMA}})_{\text{initial}} - (m_{\text{PMMA}})_{\text{final}}}{(m_{\text{PMMA}})_{\text{initial}}} \times 100 \quad (1)$$

or

$$\%C_{\text{PMMA}} = \frac{m_b - m_a}{m_b \times \omega} \times 100 \quad (2)$$

where  $m_b$  is the mass before extraction,  $m_a$  the mass after extraction and drying and  $\omega$  is PMMA weight fraction.

### 2.6. BET nitrogen adsorption

Extracted samples were cut into small pieces and submitted to the BET nitrogen adsorption technique in order to measure their specific surface area. The mean pore diameter is calculated assuming a percolation of cylinders

$$D = \frac{4V}{S} \quad (3)$$

where  $V$  is, the volume of the porosity and  $S$ , the surface area of the porosity. Mean pore diameter from BET is representative of a number average diameter. More details concerning this technique, as applied to the characterization of complex three-dimensional co-continuous structures, are given elsewhere [13].

### 2.7. Dynamic mechanical thermal analysis

Rectangular section bars were prepared at each composition for both systems by compression moulding at 230 °C and applying pressure at 1 ton (T) for 1 min, 2 T for 1 min, 3 T for 1 min and 4 T for 1 min, just after melt blending. After the moulding, the sample was quenched in cold water.

DMTA experiments were performed on a Mark II analyser from Polymer Laboratories. Samples were cut in the dimensions of 14 mm × 12 mm × 2 mm and were subjected to DMTA experiments in the two point flexural configuration at the rate of 2 °C/min with a target strain of ± 64 μm.

### 3. Results and discussion

#### 3.1. Rheology of pure materials

All pure materials studied in this work show a Newtonian plateau and a shear thinning behaviour in the frequency range from 0.01 to 1000 rad/s (Fig. 1). We calculated, for PMMA/PC1 and PMMA/PC2 systems, respectively, viscosity ratios of 0.21 and 1.38 and elasticity ratios of 0.21 and 4.22 under the mixing conditions used. Thus PC1 is 5 fold more viscous and 5 fold more elastic than PMMA. PC2 is somewhat less viscous than PMMA and 4 fold less elastic.

Moreover the torque ratios measured in the mixer are 0.33 and 1.37 for PMMA/PC1 and PMMA/PC2 systems, respectively.

#### 3.2. Morphology

It is interesting to note that PMMA/PC1 are opaque blends, from 10 to 90% of PMMA. PMMA/PC2 are transparent blends for 10 and 90% of PMMA and opaque blends from 20 to 80% of PMMA. This apparent enhancement in PMMA/PC miscibility by reducing the molecular weight

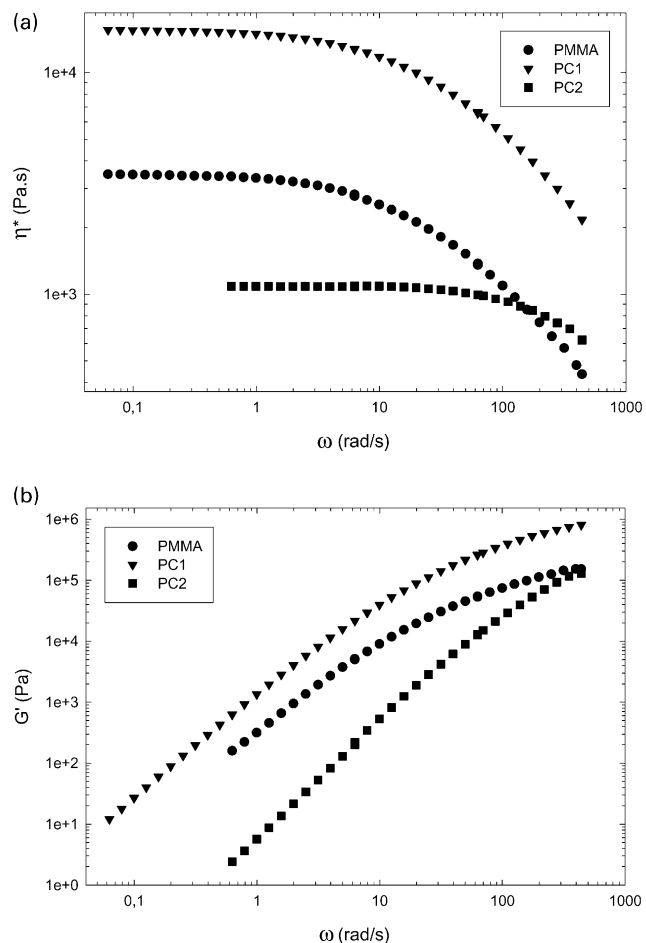


Fig. 1. Rheological properties of the pure materials. (a) Complex viscosity vs. frequency. (b) Elastic modulus vs. frequency.

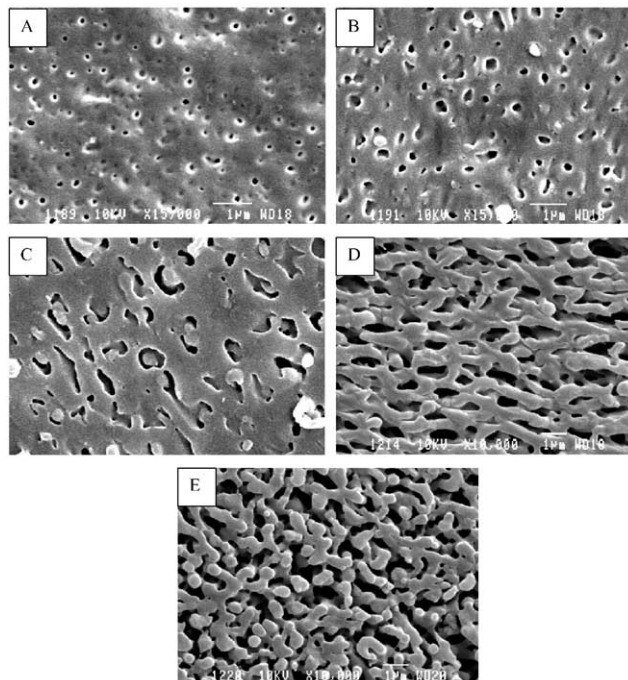


Fig. 2. Microstructure of PMMA/PC1 blends extracted with formic acid. The white bar indicates 1  $\mu\text{m}$ . (A) 20% of PMMA,  $\times 15,000$  (B) 30% of PMMA,  $\times 15,000$  (C) 40% of PMMA,  $\times 8,500$  (D) 50% of PMMA,  $\times 10,000$  (E) 60% of PMMA,  $\times 10,000$ .

of PC is consistent with lattice models predicting a greater entropy of mixing for smaller chains.

In the PMMA/PC1 system, microstructural observation via SEM indicates a dispersed phase in matrix morphology for compositions from 10 to 40% of PMMA and a co-continuous morphology for 50 and 60% (Fig. 2). Further compositions were not observed by SEM because of sample swelling during extraction.

The stronger partial miscibility of the PMMA/PC2 system compared to PMMA/PC1 system has an obvious effect on the dissolution of the PMMA. SEM observation on extracted samples indicates a film-like redeposition. This surface effect has a negligible influence on the %continuity analysis.

#### 3.3. Co-continuous morphology development

Gravimetry depicts the onset of PMMA continuity, also called the percolation threshold, between 10 and 20% of PMMA for the PMMA/PC1 system and between 20 and 30% for the PMMA/PC2 system (Fig. 3). Thus the development of PMMA continuity is situated from 10 to 40% for the PMMA/PC1 system and from 20 to 50% for the PMMA/PC2 system. Finally, the onset of full PMMA continuity to the disintegration point of the sample extracted with formic acid is situated from 50% to some composition between 70 and 80% for the PMMA/PC1 system and from 60% to some composition between 70 and 80% for the PMMA/PC2 system.



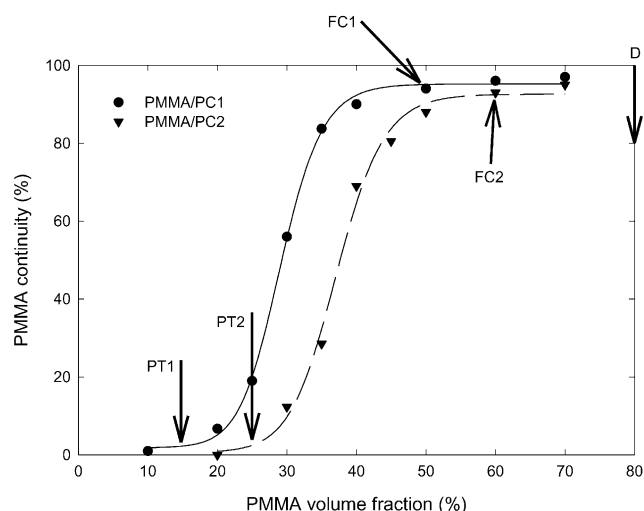


Fig. 3. Co-continuous morphology development curve: percent continuity of PMMA as a function of PMMA volume fraction. PT1 and PT2 refer to the PMMA percolation threshold values for blends with PC1 and PC2 matrix, respectively. FC1 and FC2 refer to the onset of full PMMA continuity for blends with PC1 and PC2, respectively. D refers to sample disintegration point with solvent for PMMA.

Co-continuity in a A/B system can be defined as the concentration range where both phases are 100% continuous. This is rigorously measured when selective solvents for each of the phases are available. In the case of PMMA/PC it is impossible to dissolve the PC without also dissolving out the PMMA. For this reason we define a concentration region of high continuity as existing from the onset of full continuity for PMMA, using formic acid as a solvent, to the point at which the sample disintegrates in the presence of that same solvent. Sample disintegration in formic acid is a clear indication that PMMA is the matrix and PC is the dispersed phase.

The percolation thresholds mentioned earlier are unexpectedly high for low interfacial tension systems. For instance, the Type I SEBS/HDPE system ( $\sigma = 1.0$  mN/m) reported by Li et al. [14] demonstrates a percolation threshold between 10 and 15% of dispersed phase. Secondly, the full PMMA continuity regions of these blends are relatively narrow, 50–75% for PMMA/PC1 and 60–75% for PMMA/PC2. These values are similar to that observed for high interfacial tension systems, like PS/HDPE ( $\sigma = 5.6$  mN/m) showing a full PS continuity region from 40 to 66% of PS [14]. This is quite surprising considering the very low interfacial tension of the PMMA/PC system, calculated as low as 0.6 mN/m using the harmonic mean equation and surface tensions [26]. Indeed, it is expected that the PMMA/PC system should fall into the Type I category, because of the strong interactions present and its low interfacial tension. For this reason a low percolation threshold and a broad co-continuity was expected.

For the PMMA/PC1 system, the BET nitrogen adsorption technique gives a mean pore diameter from 0.25 to 0.7  $\mu\text{m}$  for the 40–70% composition range (Fig. 4). For the

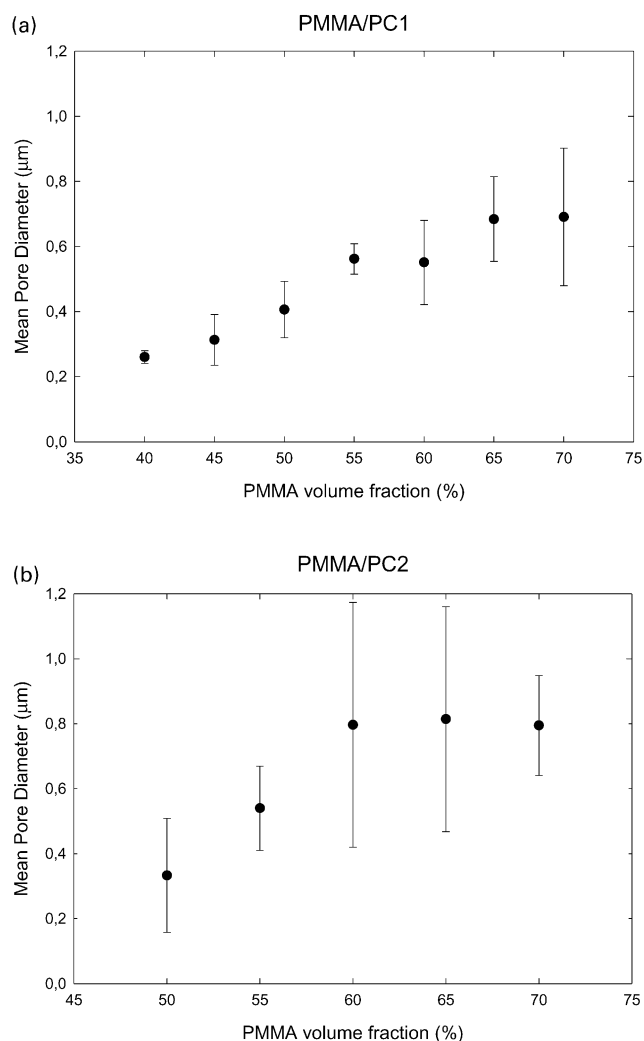


Fig. 4. BET surface area analysis of extracted blends. (a) Mean pore diameter as a function of PMMA volume fraction for the PMMA/PC1 system (b) Mean pore diameter as a function of PMMA volume fraction for the PMMA/PC2 system.

PMMA/PC2 system, the mean pore diameter is from 0.3 to 0.8  $\mu\text{m}$  for the 50–70% range. As displayed in Fig. 4, error bars indicate error as high as 50% (particularly for the PMMA/PC2 system), due to a large standard deviation based on sampling of four elements from the bulk of the blends. This is quite surprising in comparison with the low standard deviation of gravimetry results obtained from the same blends ( $< \pm 2\%$ ) and also considering that BET testing is highly reproducible ( $< \pm 5\%$ ). Partial miscibility appears to have an obvious effect on the reproducibility of melt blending. Nevertheless, the general trend is that the pore diameter increases with PMMA volume fraction.

Thus the size of microdomains in the co-continuity region, measured as the mean pore diameter of selectively extracted blends, is in the submicron range and shows a dependence on concentration. This feature is surprising, since it has been reported that low interfacial tension blends show a submicron size pore diameter in the co-continuity

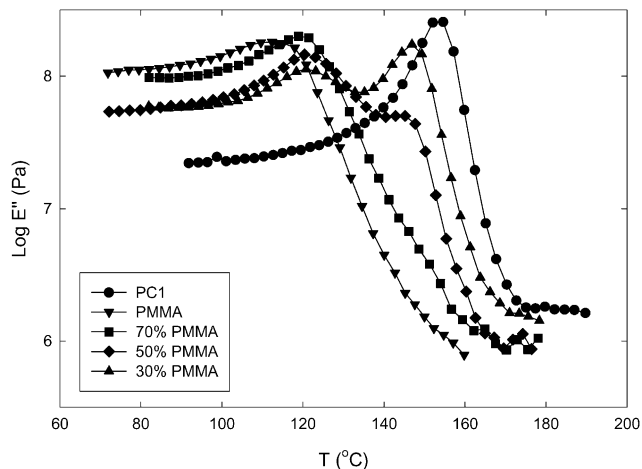


Fig. 5. Loss modulus as a function of temperature from DMTA for the PMMA/PC1 system.

region, but no concentration dependence. For instance, SEBS/HDPE Type I blends demonstrate a pore size in the 0.6  $\mu\text{m}$  range essentially independent of the composition [14].

It is clear that the PMMA/PC system does not follow typical Type I features in its continuity development as presented in Fig. 3. It will be shown in Section 3.4 that Fig. 3 needs to be corrected for partial miscibility effects.

### 3.4. Partial miscibility

The presence of two peaks in the PMMA/PC1 loss modulus scans clearly indicates two glass transitions for blends from 10 to 50% of PMMA (Fig. 5). Blends from 60 to 90% of PMMA clearly depict just one peak, related to the PMMA-rich phase glass transition, and indicate also a small shoulder, related to the PC1-rich phase glass transition. It is somewhat more difficult to extrapolate the PC1-rich phase glass transition temperature from these last compositions. Nevertheless, a glass transition temperature dependence

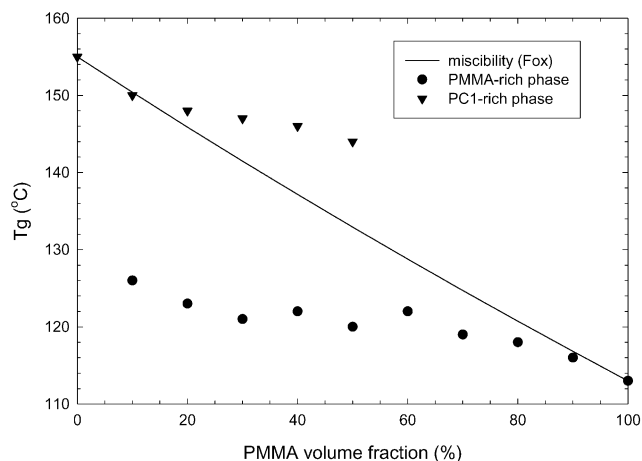


Fig. 6. Glass transition temperatures of both the PMMA-rich and the PC-rich phases as a function of PMMA volume fraction for the PMMA/PC1 system.

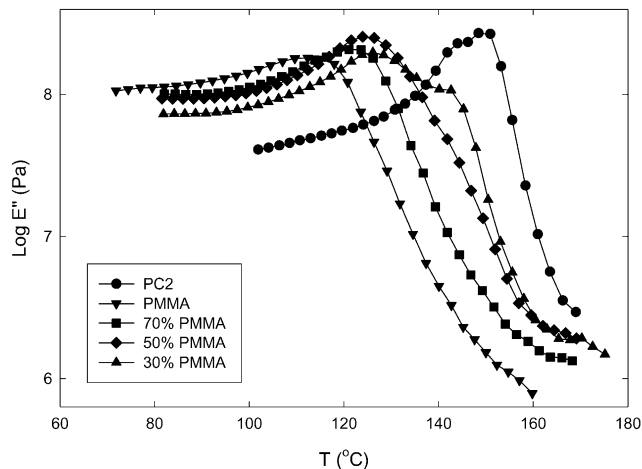


Fig. 7. Loss modulus as a function of temperature from DMTA for the PMMA/PC2 system.

with the composition is demonstrated for both phases, clearly indicating partial miscibility, that is to say the immiscibility between a PMMA-rich phase, composed of PMMA and PC1, and a PC1-rich phase, composed of PC1 and PMMA (Fig. 6). The PMMA/PC2 system shows only one peak related to the PC2-rich phase transition, for 10% of PMMA, two peaks for 20% of PMMA, one peak related to the PMMA-rich phase transition and one shoulder related to the PC2-rich phase transition, from 30 to 50% of PMMA and only one peak related to the PMMA-rich phase transition, from 60 to 90% of PMMA (Fig. 7).  $T_g$ s are also dependent on composition for this system (Fig. 8).

Using the Fox formalism, reported by Kim and Burns [17], it is possible to calculate the partial compositions of the conjugated PMMA-rich phase and PC-rich phase, that is to say the quantity of PC in the PMMA-rich phase and the quantity of PMMA in the PC-rich phase. The PC-rich phase is designated as  $'$ . The PMMA-rich phase is denoted as  $''$ ; PC as 1 and PMMA as 2. The glass transition temperatures of

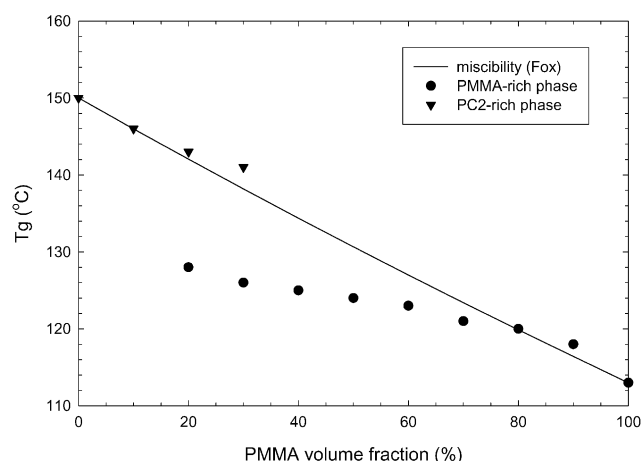


Fig. 8. Glass transition temperatures of both the PMMA-rich and the PC-rich phases as a function of PMMA volume fraction for the PMMA/PC2 system.

Table 2

Partial compositions, i.e. PMMA% in the PC-rich phase ( $\omega'_2$ ) and PC% in the PMMA-rich phase ( $\omega''_1$ ) as well as weight fraction of the rich phases, i.e. PMMA-rich phase ( $\omega''$ ) and PC-rich phase ( $\omega'$ ), for some values of total PMMA volume fraction

%PMMA	10%	20%	30%	40%	50%	60%	70%	80%	90%
<i>PMMA/PC1</i>									
$\omega'_2$	0.11	0.14	0.17	0.21	0.24	0.27	0.30	0.33	0.37
$\omega''_1$	0.30	0.28	0.25	0.23	0.20	0.17	0.15	0.12	0.10
$\omega'$	–	0.90	0.78	0.66	0.53	0.40	0.27	0.14	–
$\omega''$	–	0.10	0.22	0.34	0.47	0.60	0.73	0.86	–
<i>PMMA/PC2</i>									
$\omega'_2$	–	0.17	0.23	0.28	0.33	0.38	0.44	0.49	–
$\omega''_1$	–	0.42	0.38	0.35	0.31	0.28	0.24	0.20	–
$\omega'$	–	0.94	0.81	0.67	0.53	0.36	0.19	–	–
$\omega''$	–	0.06	0.19	0.33	0.47	0.64	0.81	–	–

the conjugated phases in the PMMA/PC partially miscible system are defined as follows

$$\frac{1}{T'_g} = \frac{\omega'_1}{T_{g1}} + \frac{\omega'_2}{T_{g2}} \quad (4)$$

and

$$\frac{1}{T''_g} = \frac{\omega''_1}{T_{g1}} + \frac{\omega''_2}{T_{g2}} \quad (5)$$

where  $\omega'_1$  is the PC wt. fraction in the PC-rich phase,  $\omega'_2$  is the PMMA wt. fraction in the PC-rich phase,  $\omega''_1$  is the PC wt. fraction in the PMMA-rich phase,  $\omega''_2$  is the PMMA wt. fraction in the PMMA-rich phase,  $T'_g$  is the glass transition temperature of the PC-rich phase,  $T''_g$  is the glass transition temperature of the PMMA-rich phase,  $T_{g1}$  is the glass transition temperature of the pure PC and  $T_{g2}$  is the glass transition temperature of the pure PMMA. The partial compositions are given by

$$\omega'_2 = \frac{T_{g2}(T_{g1} - T'_g)}{T'_g(T_{g1} - T_{g2})} \quad (6)$$

and

$$\omega''_1 = \frac{T_{g1}(T_{g2} - T''_g)}{T''_g(T_{g2} - T_{g1})} \quad (7)$$

furthermore, the immiscible phases weight fractions are expressed as

$$\omega' = \frac{\omega_2 - \omega'_2}{\omega'_2 - \omega''_2} \quad (8)$$

and

$$\omega'' = \frac{\omega_2 - \omega'_2}{\omega''_2 - \omega'_2} \quad (9)$$

where  $\omega'$  is the PC-rich phase wt. fraction in the blend,  $\omega''$  is the PMMA-rich phase wt. fraction in the blend,  $\omega_1$  is the PC wt. fraction in the blend and  $\omega_2$  is the PMMA wt. fraction in the blend.

In Table 2 the PC1 content is found to vary from 30 to 10% in the PMMA-rich phase and the PMMA content varies

from 11 to 37% in the PC1-rich phase, for the 10–90% total PMMA composition range. The PC2 content varies from 42 to 20% in the PMMA-rich phase and the PMMA content from 17 to 49% in the PC2-rich phase, for the 20–80% total PMMA composition range. PMMA appears more miscible in the PC-rich phase than the PC in the PMMA-rich phase in both systems, but this tendency is stronger for the PMMA/PC1 system. Kim and Burns [17] reported that PMMA ( $M_w = 83.7 \times 10^3$  g/mol) is more soluble in the PC-rich phase than the PC ( $M_w = 29.0 \times 10^3$  g/mol) in the PMMA-rich phase. Kolarik et al. [18] reported that PC ( $M_w = 26.0 \times 10^3$  g/mol) solubility in the PMMA-rich phase is greater than the PMMA ( $M_w = 1337 \times 10^3$  g/mol) solubility in the PC-rich phase. According to Kim and Burns and Kolarik et al. the PMMA/PC partial miscibility behaviour shows a greater solubility of PMMA in the PC-rich phase for a low PMMA/PC molecular weight ratio and the opposite for a high ratio. The tendencies observed in this study with both PMMA/PC1 and PMMA/PC2 systems are in agreement with these previous results.

Furthermore, immiscible rich phases weight fraction calculations indicate: (1) the existence of a single PC1-rich phase for the 0–12% total PMMA range, (2) the co-existence of both a PC1-rich phase and a PMMA-rich phase for the 12–90% total PMMA range, (3) the existence of a single PMMA-rich phase for the 90–100% total PMMA range (extrapolation from data of Table 2). It appears that such calculations tend to overestimate the size of the single phase regions, since the blends from 10 to 90% total PMMA were opaque (i.e. immiscible). For the PMMA/PC2 system, a single PC2-rich phase is found in the 0–15% total PMMA range. Both the PC2-rich phase and the PMMA-rich phase exist in the 15–79% total PMMA range and the range of the single PMMA-rich phase is estimated to be from 79 to 100% total PMMA (extrapolation from data of Table 2).

### 3.5. Gravimetry corrections

The partial miscibility of the PMMA/PC system involves a phase separation between both a PMMA-rich phase and a PC-rich phase and also a miscibility/immiscibility transition

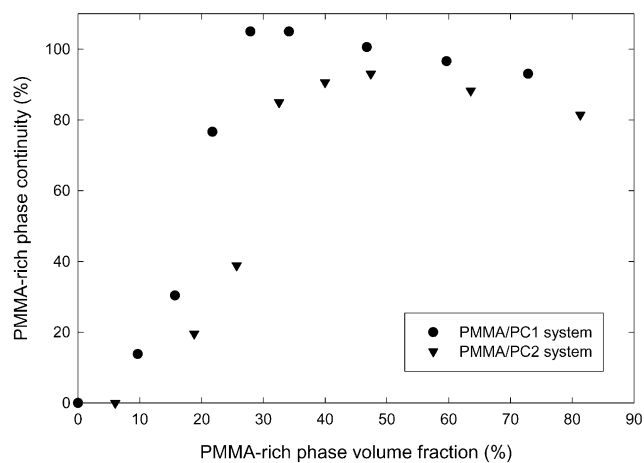


Fig. 9. Corrected co-continuous morphology development curve: percent continuity of the PMMA-rich phase as a function of PMMA-rich phase volume fraction.

at low compositions. This behaviour has an obvious effect on the morphological features of phase separated blends of PMMA and PC and especially for the co-continuous morphology development. Thus the co-continuous morphology development should be expressed in terms of a PMMA-rich phase volume fraction and PMMA-rich phase continuity. A new corrected co-continuous morphology development curve (Fig. 9) is achieved by first replacing the PMMA volume fraction by the PMMA-rich phase volume fraction and second replacing the PMMA continuity by the PMMA-rich phase continuity expressed as:

$$\%C_{\text{PMMA}} = \frac{(m_{\text{PMMA-rich phase}})_{\text{initial}} - (m_{\text{PMMA-rich phase}})_{\text{final}}}{(m_{\text{PMMA-rich phase}})_{\text{initial}}} \times 100 \quad (10)$$

or

$$\%C'' = \frac{m_b - m_a}{m_b \times \omega''} \times 100 \quad (11)$$

For the PMMA/PC1 system, the PMMA-rich phase continuity development curve demonstrates a very low percolation threshold, between 0 and 10% of PMMA-rich phase and a very broad region of full PMMA-rich phase continuity to disintegration, from 30% to some composition between 70 and 86% (sample disintegration) of PMMA-rich phase. These two main features are consistent with the essential features of Type I (binary compatible) system co-continuous morphology development as described by Li et al. [14]. It is curious to note in Fig. 4 that the pore size increases with %PMMA. This is contrary to the observations of Li et al. for highly interacting binary systems. They observed a constant pore size dependence with composition. In this system it has already been demonstrated that the partial miscibility leads to a well-separated structure at symmetrical compositions, but demonstrates miscibility at low compositions. Thus the overall quantity of

PMMA in the PC-rich phase, that is to say  $\omega_2' \times \omega_1'$ , decreases upon increasing the total amount of PMMA. As such, disproportionately more PMMA is accessible for extraction. This may affect the pore size of extracted blends as shown in Fig. 4.

The PMMA-rich phase continuity development for the PMMA/PC2 system involves a percolation threshold between 5 and 15% of PMMA-rich phase and a full PMMA-rich phase continuity to sample disintegration region from 45% to some composition between 80 and 100% (sample disintegration) of PMMA-rich phase. Once again, the percolation threshold is found to be low and the full PMMA-rich phase continuity to sample disintegration region very broad, describing typical Type I system features.

In typical purely immiscible systems it was demonstrated that the co-continuous morphology development is driven first, by the deformability of the dispersed phase during the first stage of the mixing and second, by the stability of the deformed dispersed phase during the equilibrium stage of the mixing. The deformability of the dispersed phase is given by the capillary number

$$\text{Ca} = \frac{\eta_m \dot{\gamma} R}{\sigma} \quad (12)$$

where  $\eta_m$  is the viscosity of the matrix,  $\dot{\gamma}$  the shear rate,  $R$  the radius of the droplet and  $\sigma$  is the interfacial tension. The stability of a thread is given by the time of breakup

$$t_b = \frac{2\eta_m R_0}{\Omega_m \sigma} \ln\left(\frac{0.82R_0}{\alpha_0}\right) \quad (13)$$

where  $R_0$  is the initial radius of the thread,  $\alpha_0$  the initial distortion amplitude and  $\Omega_m$  is a function related to viscosity ratio. Indeed, low interfacial tension systems experience a stable thread-like dispersed phase during the mixing in equilibrium conditions, because the thread lifetime during mixing is greater than the droplet lifetime. Such stable thread-like dispersed phases percolate through a thread–thread coalescence phenomena, requiring very low amounts of dispersed phase to build a continuous network. As a result, the co-continuous region in such systems is very broad. On the other hand, high interfacial tension systems are characterized by a droplet lifetime greater than the thread lifetime in equilibrium mixing conditions. Thus such systems demonstrate a droplet dispersed phase, requiring greater amounts of dispersed phase to percolate through droplet–droplet coalescence and resulting in a narrow co-continuous region.

Once partial miscibility has been taken into account and the gravimetry data is corrected, the PMMA/PC blend demonstrates a Type I system behaviour.

Fig. 3 indicates a shift of 10%, in the co-continuous morphology development curve, towards higher PMMA volume fraction for the PMMA/PC2 system as compared to the PMMA/PC1 system. After the gravimetry corrections, this shift is still present (Fig. 9). There are two possible



parameters which need to be discussed with respect to this shift. Firstly, PMMA/PC2 is a more highly interacting system than the PMMA/PC1 system. A more highly interacting system, with all else equal, would result in a more easily deformed thread-like dispersed phase with a higher stability. This would result in a shift in the opposite direction as to what is observed in Fig. 9. Secondly, PC2 is significantly less viscous than PC1. This would decrease the thread-like dispersed phase stability and increase the composition at which co-continuity occurs. Thus the observed shift appears to be most likely the result of the lower viscosity of the PC2 matrix material.

#### 4. Conclusion

The co-continuous morphology development curve is usually presented as the %continuity vs. the vol% fraction of the dispersed phase. By quantitatively taking into account the partial miscibility of the PMMA/PC system and correcting the solvent extraction/gravimetry data, a new co-continuous morphology development curve expressed as the %continuity vs. the vol% fraction of the PMMA-rich phase is generated. The main features of co-continuous morphology development in highly interacting polymer blends are found for the PMMA/PC system: a low percolation threshold and a broad co-continuity region. The pore size of the co-continuous extracted blends increases with composition as studied by BET analysis. It is suggested that this tendency is due to the decrease of the overall PMMA in the PC-rich phase with increasing total PMMA volume fraction. Use of a low molecular weight PC demonstrates a shift in the co-continuous morphology development curve towards higher PMMA volume fractions. This effect appears to be due to a lower dispersed phase thread stability resulting from the decrease in the matrix viscosity.

#### Acknowledgments

The authors would like to thank Dilip Odedra and Jim Chung of Bayer Inc. for their technical support and collaboration. Thanks are also due to ESTAC (Environ-

mental Science and Technology Alliance Canada) for financial support. Appreciation is also extended to Pierre Sammut of the Industrial Materials Institute of the National Research Council of Canada for his assistance with the DMTA measurements.

#### References

- [1] Avgeropoulos GN, Weissert FC, Biddison PH, Böhm GGA. *Rubber Chem Technol* 1976;49:93.
- [2] Paul DR, Barlow JW. *J Macromol Sci, Rev Macromol Chem* 1980;18:109.
- [3] Metelkin VI, Blekht VS. *Colloid J USSR* 1984;46:425.
- [4] Utracki LA. *J Rheol* 1991;35:1615.
- [5] Mekhilef N, Verhoogt H. *Polymer* 1996;37(18):4069–77.
- [6] Bourry D, Favis BD. *J Polym Sci, Part B: Polym Phys* 1998;36:1889–99.
- [7] Van Oene H. *J Colloid Interf Sci* 1972;40:448.
- [8] Willemsse RC, Posthuma de Boer A, van Dam J, Gotsis AD. *Polymer* 1998;39(24):5879–87.
- [9] Willemsse RC, Posthuma de Boer A, van Dam J, Gotsis AD. *Polymer* 1999;40:827–34.
- [10] Mekhilef N, Favis BD, Carreau PJ. *J Polym Sci, Part B: Polym Phys* 1997;35:293–308.
- [11] Veenstra H, van Dam J, Posthuma de Boer A. *Polymer* 1999;40:1119–30.
- [12] Willemsse RC. *Polymer* 1999;40:2175–8.
- [13] Li J, Favis BD. *Polymer* 2001;42:5047.
- [14] Li J, Ma P, Favis BD. *Macromolecules* 2002;35:2005–16.
- [15] Gardlung ZG. *Polym Prepr (Am Chem Soc, Div Polym Chem)* 1982;23:258.
- [16] Koo K-K, Inoue T, Miyasaka K. *Polym Engng Sci* 1985;25(12):741–6.
- [17] Kim WN, Burns CM. *Macromolecules* 1987;20(8):1876–82.
- [18] Kolarik J, Lednický F, Pukanszky B, Pegoraro M. *Polym Engng Sci* 1992;32(13):886–93.
- [19] Gardlung ZG. *Polymer blends and composites in multiphase systems. Advances in chemistry series no. 206. Washington, DC: CD Han Edition; 1984. Chapter 9.*
- [20] Chiou JS, Barlow JW, Paul DR. *J Polym Sci, Part B: Polym Phys* 1987;25:1459–71.
- [21] Saldanha JM, Kyu T. *Macromolecules* 1987;20(11):2840–7.
- [22] Kyu T, Saldanha JM. *J Polym Sci, Part C: Polym Lett* 1988;26:33–40.
- [23] Kyu T, Saldanha JM. *Macromolecules* 1988;21(4):1021–6.
- [24] Nishimoto M, Keskkula H, Paul DR. *Polymer* 1991;32(2):272–8.
- [25] Yang L-Y, Bigio D, Smith TG. *J Appl Polym Sci* 1995;58:129–41.
- [26] Brandrup J, Immergut EH. *Polymer handbook, 3rd ed. New York: Wiley; 1989.*